

Fiber Laser-Generated Silver-109 Nanoparticles for Laser Desorption/Ionization Mass Spectrometry of Illicit Drugs

Zuzanna Krupa and Joanna Nizioł*

Cite This: *J. Am. Soc. Mass Spectrom.* 2024, 35, 1156–1167

Read Online

ACCESS |



Metrics & More



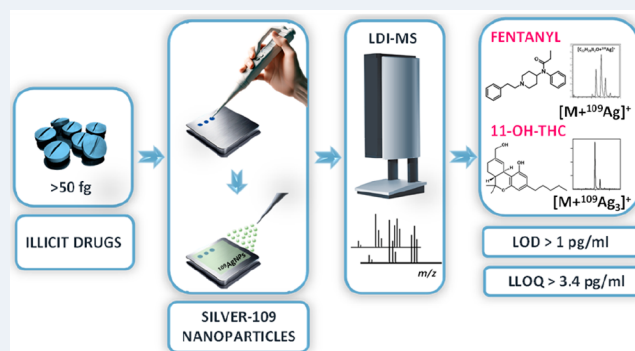
Article Recommendations



Supporting Information

ABSTRACT: Cannabinoids and opioids are the most prominently used drugs in the world, with fentanyl being the main cause of drug overdose-related deaths. Monitoring drug use in groups as well as in individuals is an important forensic concern. Analytical methods, such as mass spectrometry (MS), have been found most useful for the identification of drug abuse on a small and large scale. Pulsed fiber laser 2D galvoscaner laser-generated nanomaterial (PFL 2D GS LGN) was obtained from monoisotopic silver-109. Nanomaterial was used for laser desorption/ionization mass spectrometry of selected illicit drug standards with standard high-resolution reflectron-based time-of-flight MALDI apparatus. Δ^9 -THC, 11-OH-THC, 11-COOH-THC, fentanyl, codeine, 6-monoacetylmorphine (6-MAM), heroin, tramadol, and methadone were chosen as test compounds. Illicit drugs were tested in a concentration range from 100 $\mu\text{g}/\text{mL}$ to 10 pg/mL , equating to 50 μg to 50 fg per measurement spot. For all analyzed compounds, identification and quantification by silver-109-assisted laser desorption/ionization (LDI) MS was possible, with uncommon $[M + ^{109}\text{Ag}_3]^+$ and $[M - H]^+$ ions present for certain structures. The results of the quantitative analysis of drugs using silver-109 PFL 2D GS LGN for LDI MS are presented. Laser-generated NPs are proven to be useful for the analysis of selected drugs, with exceptionally good results for fentanyl monitoring in a broad range of concentrations.

KEYWORDS: *cannabinoids, opioids, monoisotopic silver nanoparticles, mass spectrometry quantification*



1. INTRODUCTION

According to the United Nations Office on Drugs and Crime (UNODC) global estimates of the prevalence of drug use in 2021, the use of opioids, including opiates and prescription opioids, was determined to be 1.18% of the world population (0.72, 1.49),¹ which makes it over 3 times higher than in 2017.² The term opioids refers to exogenous compounds, both natural and synthetic, which bind to opioid receptors. Natural opiates, i.e. codeine, are obtained from the poppy plant as alkaloids constituting a substance known as opium.³ The remaining opioids analyzed in this paper are either of synthetic or semisynthetic origin and metabolites. Among them, fentanyl continues to be the drug of choice due to being relatively easy to produce but most importantly having a high potency, 100 times higher than morphine.⁴ The epidemic of fentanyl-induced overdose deaths in the United States started around the year 2015 with 9580 deaths connected to this cause and reached its first peak in 2017, amounting to 28 466 deaths. Since then, as of 2021, the amount of overdose-induced deaths caused by synthetic opioids, primarily fentanyl, increased roughly 2.5 times, with 70 601 deaths.^{5,6} In contrast, the European Monitoring Centre for Drugs and Drug Addiction (EMCDDA)

reports 49 confirmed deaths linked to fentanyl, with a minimum estimate of 137 deaths overall in Europe in the year 2021.⁷

Opioid use is the second most prevalent illicit drug use reported by UNODC, the first one being cannabis at 4.27% (3.08, 5.38). The most distinctive class of compounds found in cannabis plants are cannabinoids.⁸ A part of this group, Δ^9 -tetrahydrocannabinol (Δ^9 -THC), is considered as the main compound contributing to the psychoactive effect of cannabis use. THC is metabolized in the human body, resulting in the formation of 11-hydroxy- Δ^9 -THC (11-OH-THC) and 11-nor-9-carboxy- Δ^9 -THC (11-COOH-THC).⁹

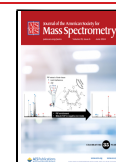
Mass spectrometry (MS) coupled with liquid (LC) or gas chromatography (GC) is currently the most widespread analytical technique for illicit drug identification. Several research studies focus on employing LC-MS in estimating illicit drug use in a population rather than in an individual. One of

Received: December 27, 2023

Revised: April 24, 2024

Accepted: April 26, 2024

Published: May 6, 2024



those approaches is sewage forensics, which focuses on analyzing samples of wastewater from certain living areas.^{10–12} For fast identification of illicit drugs in a specific suspect of drug use, approaches such as fluorescence-based lateral flow assay for THC detection in the saliva are used.¹³ Another more conclusive technique is electrochemical detection, with a broad spectrum of solutions for various drugs, giving the possibility of testing oral fluids¹⁴ or seized powders.¹⁵

Table 1. List of Identified Ions with Mean Signal Intensity and Signal-to-Noise Ratios of Analyzed Compounds at 100 $\mu\text{g}/\text{mL}$ Concentration

compound	ion type	mean intensity	S/N
11-OH-THC	[M + H] ⁺	1024	7.7
	[M + Na] ⁺	3107	26.5
	[M + ¹⁰⁹ Ag] ⁺	26498	298.8
	[M + ¹⁰⁹ Ag ₃] ⁺	8568	333.1
11-COOH-THC	[M + H] ⁺	1102	9.3
	[M + ¹⁰⁹ Ag] ⁺	17908	228.9
	[M + ¹⁰⁹ Ag ₃] ⁺	3202	83.9
THC fentanyl	[M + ¹⁰⁹ Ag] ⁺	398	7.7
	[M + H] ⁺	6835	110.3
codeine	[M + Na] ⁺	830	15.2
	[M + ¹⁰⁹ Ag] ⁺	18285	479.8
	[M + H] ⁺	863	18.4
	[M + Na] ⁺	829	14.6
	[M + K] ⁺	369	6.6
6-MAM	[M + ¹⁰⁹ Ag] ⁺	851	22.6
	[M – H] ⁺	10158	190.5
	[M + H] ⁺	2154	16.4
	[M + Na] ⁺	660	7.3
	[M + ¹⁰⁹ Ag] ⁺	1912	29.4
heroin	[M – H] ⁺	8887	119.8
	[M + H] ⁺	1678	18.7
	[M + Na] ⁺	1687	20.3
	[M + ¹⁰⁹ Ag] ⁺	7241	124.2
tramadol	[M – H] ⁺	8286	120.2
	[M + H] ⁺	692	7.2
	[M + ¹⁰⁹ Ag] ⁺	5452	101.7
methadone	[M – H] ⁺	11161	151.4
	[M + H] ⁺	2894	32.0

In this study, the applied analytical method allowed for rapid screening for fentanyl and other illicit drugs. The sample preparation for ¹⁰⁹AgNP-assisted LDI MS is a matter of minutes, with the spectral data acquisition itself taking even less time.^{16–18} Recently, our research has successfully applied this technique for both qualitative and quantitative analysis of low molecular weight compounds, including amino acids,^{17–19} carboxylic acids,^{20–24} and hormones.²⁵ Furthermore, this method has shown exceptional utility in analyzing microorganisms^{26–29} and various human biological samples such as serum,³⁰ urine,^{30,31} and tissue. Notably, we have showcased its significant potential in mass spectrometry imaging (MSI), particularly in creating detailed molecular imprints of plant^{32,33} and human tissues.^{34–36} The resulting limit of detection for fentanyl acquired using silver-109-assisted LDI MS analysis illustrates the advantages of the method for the identification and quantification of fentanyl.

2. MATERIALS AND METHODS

2.1. Materials. All drugs were obtained from Sigma-Aldrich. The steel target was machined from H17 (1.4016) stainless steel. The steel target was cleaned by soaking in boiling solvents: toluene (3 × 100 mL for 30 s), chloroform (3 × 100 mL for 30 s), acetonitrile (3 × 100 mL for 30 s), and deionized water (3 × 100 mL for 30 s) before further use. The plate was dried in a high vacuum (ca. 0.01 mbar, 24 h). Solvents in use were of LC-MS grade, apart from water (18 M Ω -cm water produced locally).

2.2. PFL 2D GS Laser-Generated Nanomaterial (LGN) of Silver-109. Silver-109 foil used to produce nanoparticles (~1 mm thick, 99.7% isotopic purity) was bought from Trace Sciences International (USA). The foil was placed in a glass vessel and covered by acetonitrile, with a total solvent volume of 3 mL.

Laser ablation was conducted with a 1064 nm pulsed fiber laser (Raycus RFL-P20QE/A3). The ¹⁰⁹AgNPs suspension was prepared by 2 min of irradiation, with pulse energy of 0.8 mJ (100 ns pulse length) at a repetition rate of 40 kHz and scanning speed of 2000 mm/s. The ablation area was 4 × 4 mm. Suspension was transferred into a syringe immediately after ablation and used in the nebulization step.

2.3. Nebulization of ¹⁰⁹AgNPs Suspension. The nebulization process was controlled by dedicated software. The H17 steel plate was placed on the table of a translation system consisting of a motorized XY table powered by closed-loop servomotors. A glass syringe (1 mL) was filled with the suspension of silver-109 nanoparticles prepared earlier and placed in a syringe pump (250 $\mu\text{L}/\text{min}$). The 2D system table was directed by custom-made software with 10 mm/s translation speed using a sequence of movements prepared to uniformly cover a target plate. The nebulizer was a typical, standard flow Bruker ion source nebulizer. Argon at a pressure of 2 bar was used as the nebulizing gas. Studied standards were placed on the target plate before nebulization with an automatic pipet.

2.4. Standard Sample Preparation. Each compound standard was diluted with methanol to give a final concentration of 100 $\mu\text{g}/\text{mL}$. Lower concentrations were prepared by further dilution of ten-times higher concentration ones. Volumes of 0.5 μL (¹⁰⁹AgNPs) of selected drug solutions were placed directly on the target plate. After air drying, the target was covered with ¹⁰⁹AgNPs suspension as stated previously.

2.5. Human Sample Preparation. The serum and urine samples were obtained from a healthy volunteer during a medical examination conducted at Hospital John Paul II in Kolbuszowa, Poland, with the purpose of detecting urinary tract malignancies. The research project received approval from the Local Bioethics Committee of the University of Rzeszów (Poland), with permit number 2018/04/10. The study was carried out in compliance with relevant rules and legislation. A volume of approximately 2.6 mL of blood was obtained from the patient and thereafter subjected to centrifugation at a speed of 3000 rpm for a duration of 10 min at ambient temperature. Blood workup was performed in the hospital and by a legally entitled medical professional working in the hospital. The serum was subsequently isolated and preserved at a temperature of –80 °C until it was needed again. Blood serum and urine were diluted 500-times with ultrapure water, and then 100 μL of serum or urine or an equal volume of previously prepared fentanyl standard solutions in concentrations of 100 $\mu\text{g}/\text{mL}$ to 10 pg/mL was added, resulting in concentrations of fentanyl in spiked

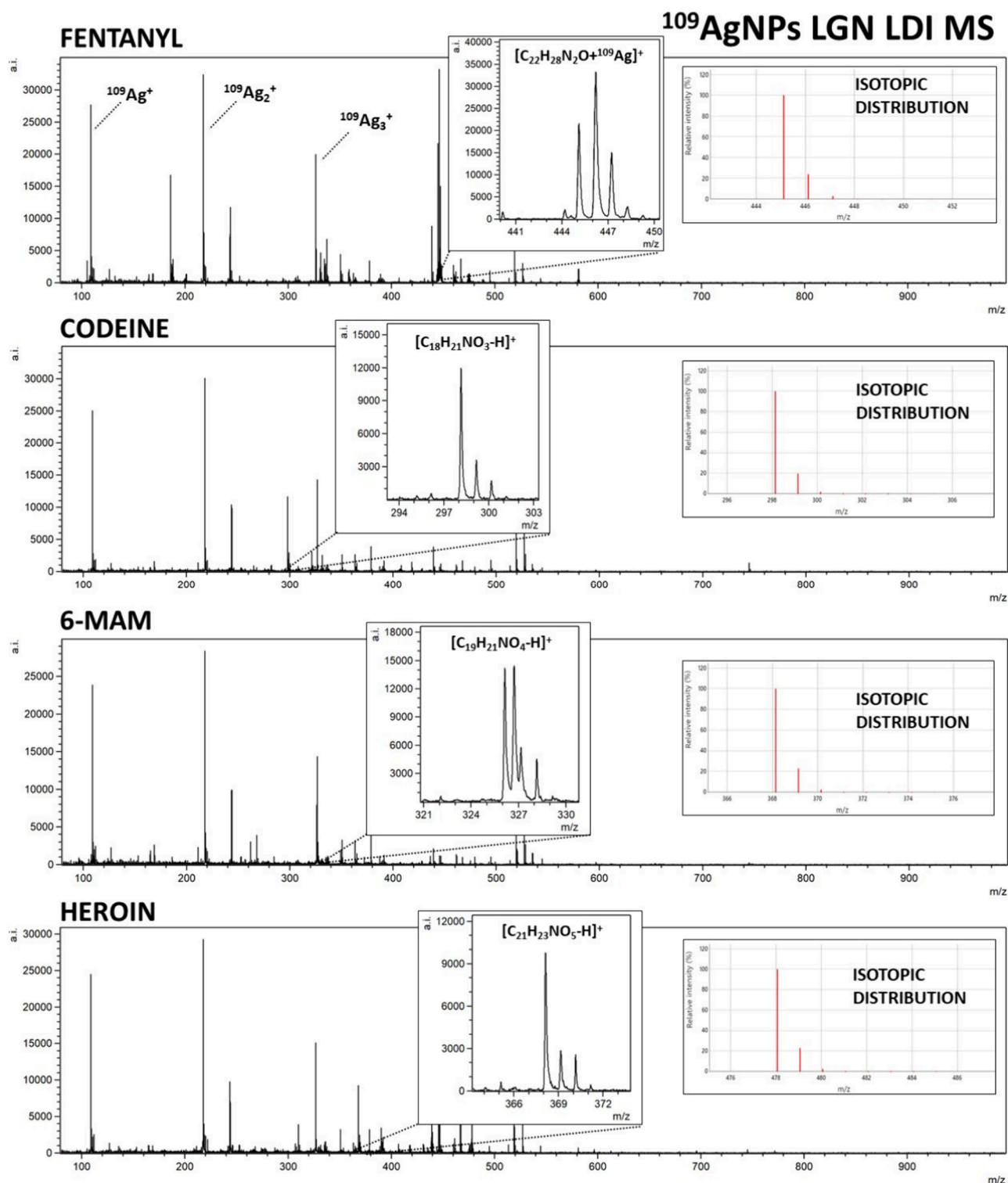


Figure 1. Mass spectra of opioids: fentanyl, codeine, 6-monoacetylmorphine (6-MAM), and heroin, obtained by ^{109}Ag -assisted LDI MS. The spectra correspond to a sample concentration of $100\ \mu\text{g/mL}$, equating to $50\ \text{ng}$ of compound per measurement spot. Selected identified ions and their calculated isotopic distributions are presented on the spectra.

samples from $50\ \mu\text{g/mL}$ to $5\ \text{pg/mL}$. The obtained samples were placed directly on a steel target plate ($0.5\ \mu\text{L}$ per spot) previously coated with $^{109}\text{AgNPs}$.

2.6. LDI Mass Spectrometry. Laser desorption/ionization–time-of-flight (LDI-ToF) mass spectrometry experiments were performed in reflectron mode using a Bruker Autoflex Speed time-of-flight mass spectrometer equipped with a

SmartBeam II laser ($352\ \text{nm}$). Laser impulse energy was approximately $100\ \mu\text{J}$, and the laser repetition rate was $1000\ \text{Hz}$. The total number of laser shots was 9000 for each spot. This amount of laser shots was divided into three, the points positioned at a distance of ca. $1/3$ of the spot radius from its center. At each point, 3000 laser shots were made with default random walk applied. The measurement range was $m/z\ 80$ –

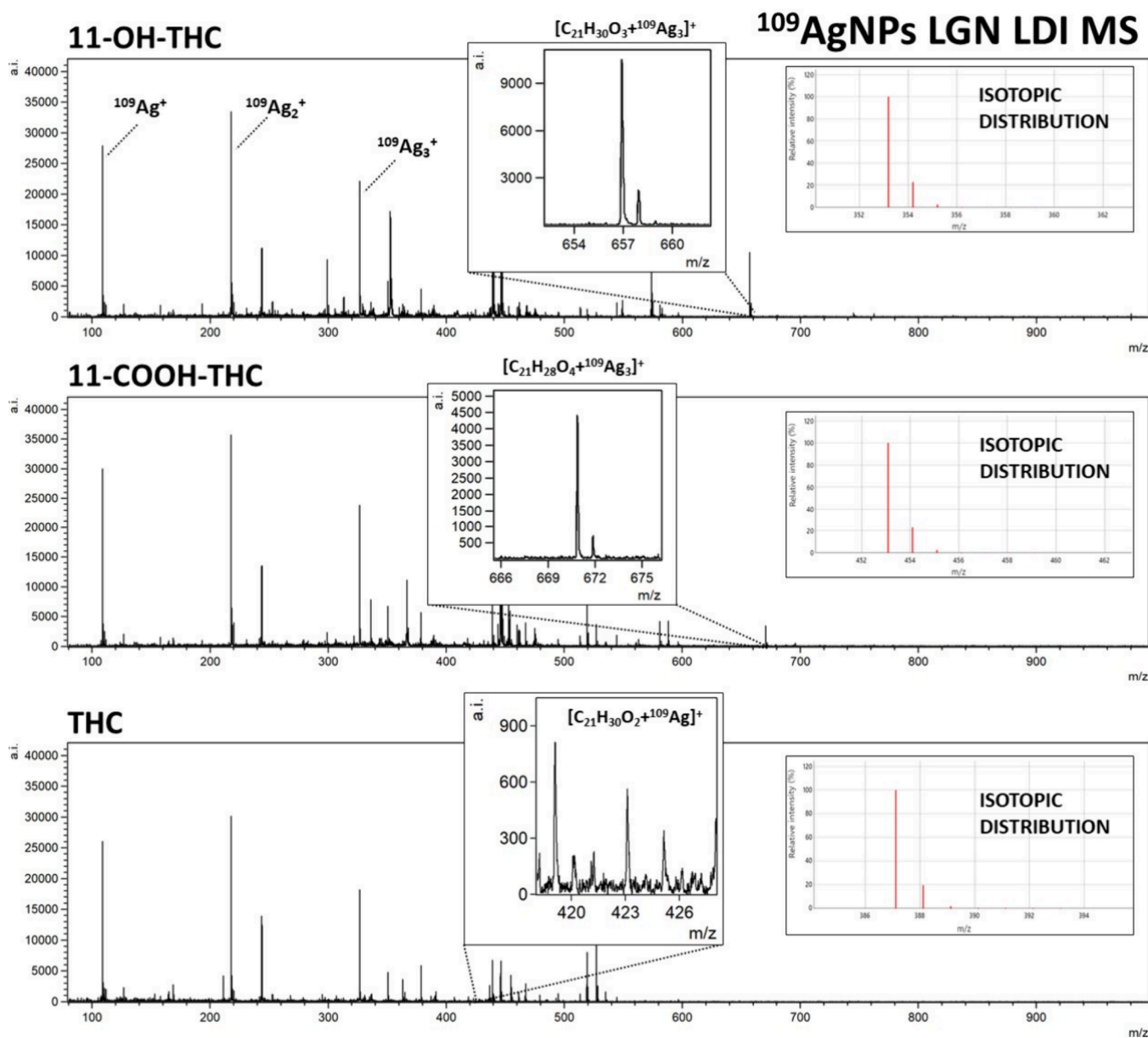


Figure 2. Mass spectra of THC and its metabolites, 11-OH-THC, and 11-COOH-THC, obtained by ^{109}Ag -assisted LDI MS. The spectra correspond to a sample concentration of $100\ \mu\text{g/mL}$, equating to $50\ \text{ng}$ of compound per measurement spot. Selected identified ions and their isotopic distributions are presented on the spectra.

1000. Suppression was turned on typically for ions of m/z lower than 80. Reflector voltages used were 21 kV (the first) and 9.55 kV (the second). The data were calibrated and analyzed with FlexAnalysis (version 3.3) using a centroid calibration model. Mass calibration was performed using internal standards (silver-109 ions and clusters from $^{109}\text{Ag}^+$ to $^{109}\text{Ag}_9^+$).

3. RESULTS AND DISCUSSION

In this research, the applicability of $^{109}\text{AgNPs}$ -assisted laser desorption/ionization MS for identification and quantification of fentanyl and other drugs, such as THC and its two metabolites, as well as opioids, including tramadol, 6-monoacetylmorphine (6-MAM), codeine, methadone, and heroin, was presented. Silver-109 nanoparticle-enhanced LDI applicability for samples of various compositions has been presented by our team in the past.^{19,21,25} Obtained mass spectra are presented in Figures 1–3. The list of identified ions with the

average signal intensity and signal-to-noise ratio of the analyzed compounds at a concentration of $100\ \mu\text{g/mL}$ is presented in Table 1.

For all of the analyzed opioids, except methadone, $[\text{M} + ^{109}\text{Ag}]^+$ ions were identified in corresponding spectra, which further confirms the validity of silver-109-nanoparticle-assisted LDI as an effective analytical method. Especially high signal intensity has been observed for $[\text{fentanyl} + ^{109}\text{Ag}]^+$ adduct ions, as well as for $[\text{11-OH-THC} + ^{109}\text{Ag}]^+$ (Figure 1) and $[\text{11-COOH-THC} + ^{109}\text{Ag}]^+$ (Figure 2). Nonetheless, the mass spectra of codeine, heroin, 6-MAM, and tramadol allowed for the identification of $[\text{M} - \text{H}]^+$ ions of significantly higher intensities than $[\text{M} + ^{109}\text{Ag}]^+$ ions of the given sample (Figures 1 and 3). The formation of deprotonated ions with positive charge is characteristic for tertiary amines. It is believed to be a result of photoionization caused by the UV laser used in the MALDI MS ion source. The mechanism of this process is explained as the

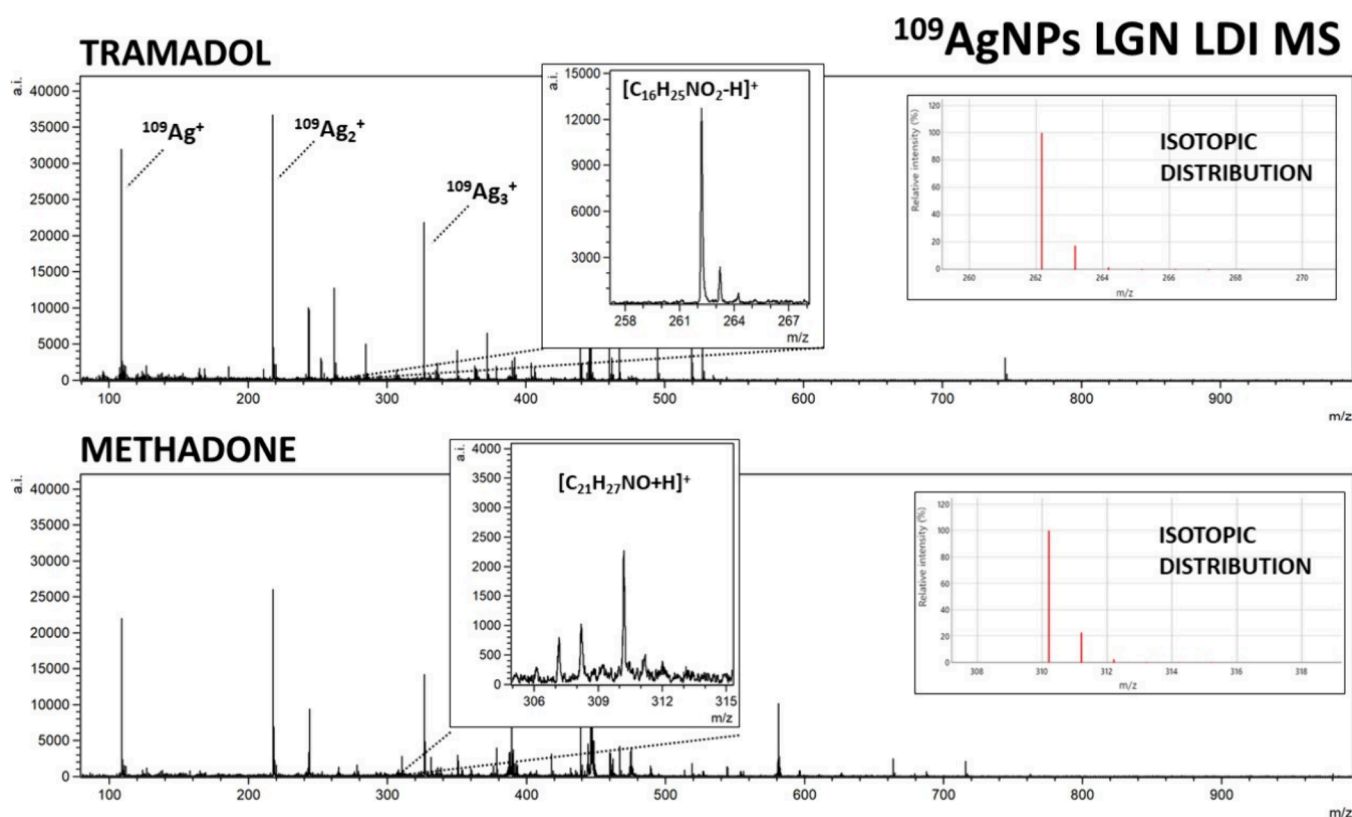


Figure 3. Mass spectra of tramadol and methadone obtained by ^{109}Ag -assisted LDI MS. The spectra correspond to a sample concentration of $100\ \mu\text{g}/\text{mL}$, equating to $50\ \text{ng}$ of compound per measurement spot. Selected identified ions and their isotopic distributions are presented on the spectra.

Table 2. Limits of Detection (LOD), Limits of Quantification (LOQ), and Linearity R^2 for Tested Compounds

compound	LOD	LLOQ	R^2
11-OH-THC	$538.92 \pm 207.47\ \text{ng}/\text{mL}$	$1796.41 \pm 691.57\ \text{ng}/\text{mL}$	0.97
11-COOH-THC	$6671.61 \pm 202.18\ \text{ng}/\text{mL}$	$22238.7 \pm 6739.38\ \text{ng}/\text{mL}$	0.96
THC	$39.13 \pm 20.76\ \mu\text{g}/\text{mL}$	$130.43 \pm 69.23\ \mu\text{g}/\text{mL}$	0.98
fentanyl	$1.03 \pm 0.19\ \text{pg}/\text{mL}$	$3.43 \pm 0.66\ \text{pg}/\text{mL}$	0.98
codeine	$61.22 \pm 8.7\ \text{ng}/\text{mL}$	$204.08 \pm 29.01\ \text{ng}/\text{mL}$	0.94
6-MAM	$57.14 \pm 10.16\ \text{ng}/\text{mL}$	$190.48 \pm 33.87\ \text{ng}/\text{mL}$	0.97
heroin	$8.22 \pm 0.16\ \text{ng}/\text{mL}$	$27.4 \pm 0.53\ \text{ng}/\text{mL}$	0.86
tramadol	$44.55 \pm 29.98\ \text{ng}/\text{mL}$	$148.51 \pm 99.92\ \text{ng}/\text{mL}$	0.99
methadone	$386.27 \pm 8.93\ \text{ng}/\text{mL}$	$1287.55 \pm 297.51\ \text{ng}/\text{mL}$	0.96

initial protonation of the N atom, followed by deprotonation and formation of the $\text{C}=\text{N}$ double bond.^{37,38}

For THC and its metabolites, 11-OH-THC and 11-COOH-THC, the most prominent identified ion was $[\text{M} + ^{109}\text{Ag}]^+$, with $[\text{M} + \text{H}]^+$ (for OH-THC and COOH-THC) and $[\text{M} + \text{Na}]^+$ (for OH-THC) also identifiable (Figure 2). Peaks of significant intensity corresponding to rarely appearing triatomic silver-109 cation adducts $[\text{M} + ^{109}\text{Ag}_3]^+$ were also present for the two THC metabolites. Mentioned adducts have been recorded previously for amino acids³⁹ and other compounds.⁴⁰ While a distinct occurrence of those adducts has been documented previously for codeine,⁴¹ the $[\text{codeine} + ^{109}\text{Ag}_3]^+$ peak on the mass spectrum acquired in this research was not of significant intensity. An assumption can be made that the occurrence of $[\text{M} + ^{109}\text{Ag}_3]^+$ ions has little correlation with the nature of the compound, rather depending on the conditions of the analysis. Sodium and potassium adducts were also identified for selected samples as presented in Table 1.

3.1. Quantification Results. The measurements of analyzed standards were performed in the concentration range from $100\ \mu\text{g}/\text{mL}$ to $10\ \text{pg}/\text{mL}$. Samples were placed on the target plate in a $0.5\ \mu\text{L}$ volume equating to $50\ \text{ng}$ to $50\ \text{fg}$ of compound per spot. The limit of detection (LOD) was calculated based on the S/N ratio of the highest intensity adduct monoisotopic signal of 3, obtained from the mass spectra of the lowest concentration from each sample. The lower limit of quantification (LLOQ) was calculated using an S/N ratio of 10. A regression analysis of mean intensity as a function of sample concentration was conducted. The LOD, LLOQ results, and R^2 values for the linear regressions of the tested compounds are presented in Table 2.

Figure 4 presents the relations of all identified adduct ions' signal intensities against the concentration of the compound in the sample. For Δ^9 -THC, the average signal intensity values were rather low, which might cause the quantification of said compound in lower concentrations to be unattainable. Nevertheless, both THC metabolites showed sufficient signal

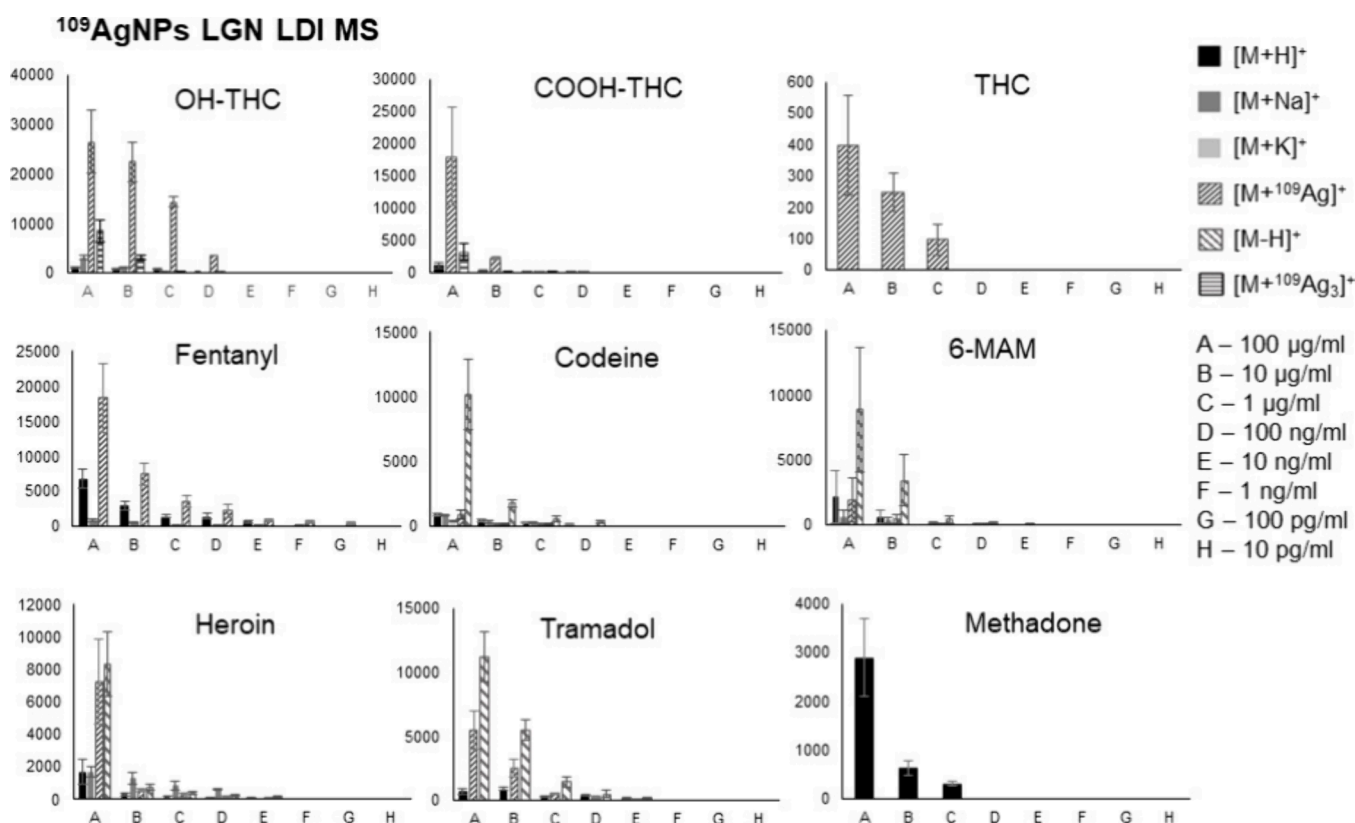


Figure 4. Relation of the mean intensity of adduct ions versus sample concentration, along with standard deviation for each measuring spot presented as bar charts for all tested compounds.

intensity, which suggests that the method might be suitable for the detection of THC-containing drug usage in humans in connection with the reasons stated previously. The results for most of the analyzed standards indicate that using ¹⁰⁹AgLGN for LDI MS has its usefulness in illicit drug identification and quantification within the used sample concentration range, making it suitable for regression analysis.

Figure 5 shows bar charts with corresponding linear regression functions. In the case of OH-THC and COOH-THC the [M + ¹⁰⁹Ag₃]⁺ adducts were chosen for analysis; for THC and fentanyl, the [M + ¹⁰⁹Ag]⁺ ions were used, for methadone, [M + H]⁺ was the selected adduct ion, and for codeine, 6-MAM, heroin, and tramadol the [M – H]⁺ ions were the most suitable. Additionally, Figures 6 and 7 present the selected ions of each analyzed compound, showcasing the decrease in signal intensity.

The first analyzed opioid was fentanyl, a synthetic analgesic. Despite structurally having traits of a tertiary amine, no significant signal intensities of [M – H]⁺ ion were observed for said compound. Regardless of that, an exceptional result was obtained for the [C₂₂H₂₈N₂O + ¹⁰⁹Ag]⁺ adduct ion. A logarithmic relationship between intensity and concentration was found for almost all analyzed concentrations, except the lowest one, in a range of 100 µg/mL to 100 pg/mL. LOD value was found to be 1.03 pg/mL (0.515 fg/per spot). The coefficient of determination found for acquired data was 0.98 (Figure 5 A). In the work of Angi et al. from 2019,⁴² the UHPLC method coupled with single quadrupole mass spectrometry was used to determine 19 fentanyl analogues also using standard solutions diluted with methanol. The authors managed to obtain a LOD of 3 ng/mL for fentanyl. The LOD in this current research is

approximately 3000 times lower than that reported in the LC-MS method, suggesting that ¹⁰⁹AgNP-assisted LDI MS is a powerful method of screening for fentanyl.

The 11-OH-THC adduct ion [C₂₁H₃₀O₃ + ¹⁰⁹Ag₃]⁺ was identified in the four highest concentrations, from 100 µg/mL to 100 ng/mL. LOD was calculated to be 0.54 µg/mL (270 pg/per spot). As presented in Figure 5B, the linear regression function gave the coefficient of determination R² value of 0.97. For 11-COOH-THC, the triatomic silver cation adduct was also chosen for the regression analysis. The [C₂₁H₂₈O₄ + ¹⁰⁹Ag₃]⁺ ion was found in the three highest sample concentrations, from 100 µg/mL to 1 µg/mL. LOD was found to be 6.67 µg/mL (3.34 ng/per spot). The R² value calculated by the regression analysis of this compound is 0.96 as seen in Figure 5B. For Δ⁹-THC, only [C₂₁H₃₀O₂ + ¹⁰⁹Ag]⁺ adduct ion has shown the logarithmic relationship of intensity on concentration. It was found in the three highest concentrations. The LOD value was calculated to be 39.13 µg/mL (19.57 ng/per spot) and the R² value was determined as 0.98. Referring to the previously mentioned study from Heo et al.,⁴³ the LOD and LOQ determined for THC were respectively 0.6 ng/mL and 0.0018 in methanol-diluted standard samples using UPLC–MS/MS with a triple quadrupole detector. The corresponding coefficient of determination was 0.9999. In the research conducted by Simões et al.,⁴⁴ the LOD values obtained from the calibration curve for standard solutions dissolved in methanol were 0.5 ng/mL for 11-OH-THC and THC-COOH and 0.5 ng/mL for THC.

Codeine, naturally found in opium poppy produced the highest intensity ion assigned to [C₁₈H₂₁NO₃ – H]⁺ formula. It was identified as the four highest concentrations. The limit of detection calculated for codeine was 61.22 ng/mL (30.6 pg/per

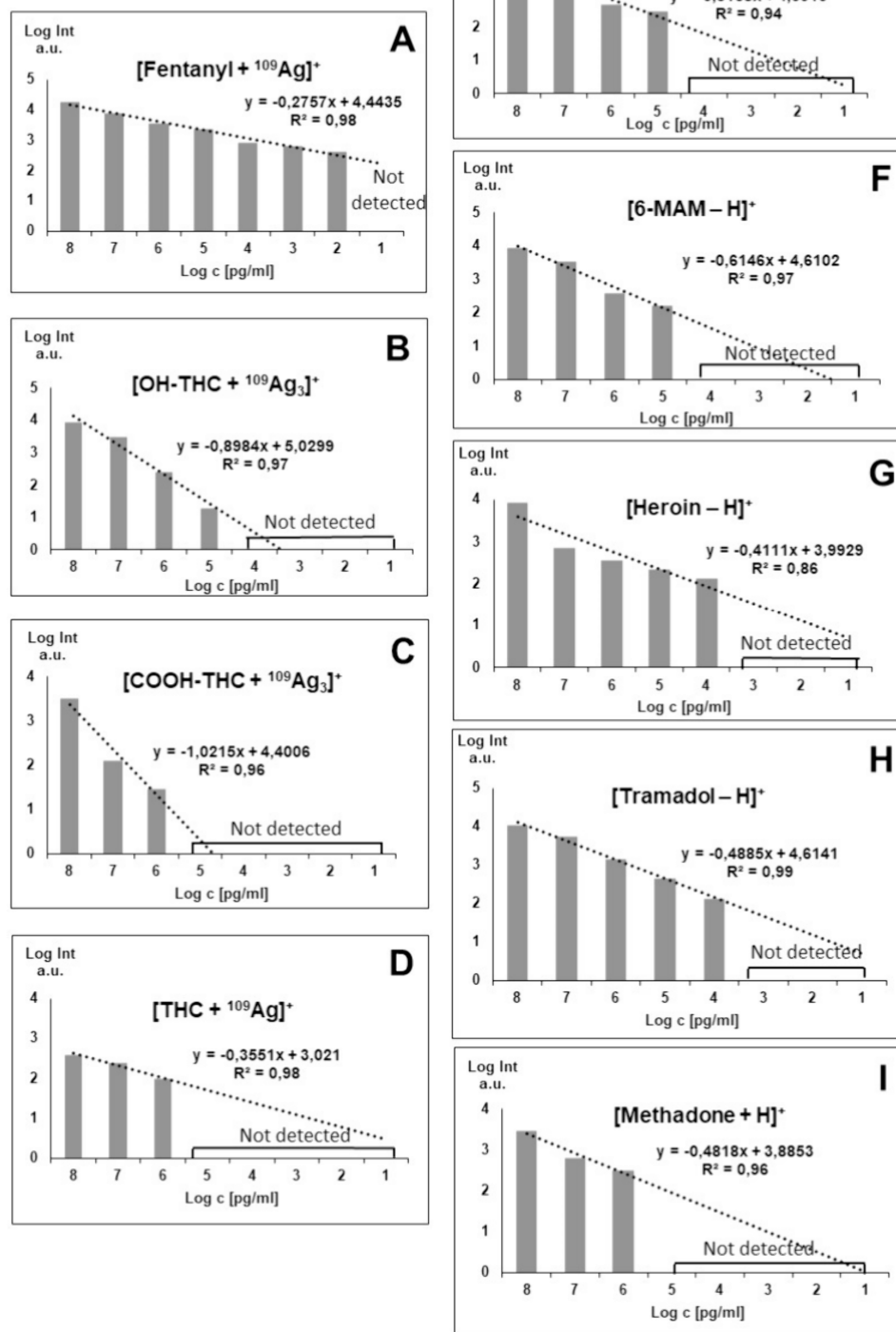
$^{109}\text{AgNPs}$ LDI MS

Figure 5. Bar charts presented for the relation of logarithm of signal intensity against the logarithm of concentration, along with regression lines and equations for A: fentanyl, B: 11-OH-THC, C: 11-COOH-THC, D: Δ^9 -THC, E: codeine, F: 6-monoacetylmorphine, G: heroin, H: tramadol, I: methadone.

spot). The R^2 value was found to be 0.94. For 6-monoacetylmorphine, which is a metabolite of heroin, a logarithmic relationship of intensity versus concentration was found for the 100 $\mu\text{g}/\text{mL}$ to 100 ng/mL range. The ion used for regression analysis was $[\text{C}_{19}\text{H}_{21}\text{NO}_4 - \text{H}]^+$. LOD calculated by using the signal-to-noise ratio was found to be 57.14 ng/mL

(28.57 $\text{pg}/\text{per spot}$). The bar chart used for the analysis of regression is presented in Figure 4F, with an R^2 value of 0.97. In research conducted in 2016 by Gul et al.⁴⁵ regarding the analysis of opiates in wastewater using LC-MS/MS, the LOD and LOQ values determined for standard solutions of codeine and 6-MAM were 0.62 ng/mL with an R^2 coefficient of 0.9998.

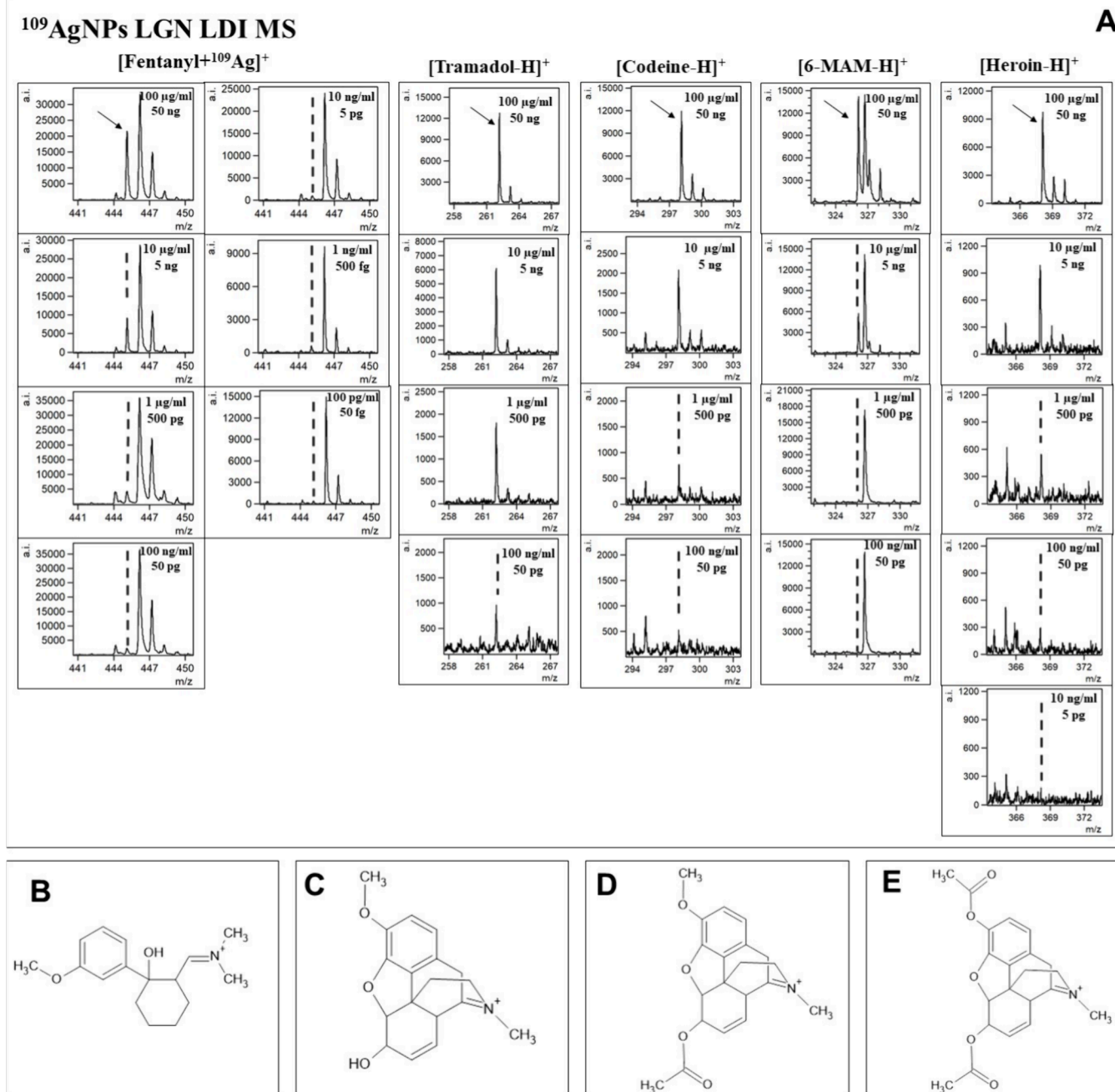


Figure 6. A: Spectra fragments for selected ions of interest presented for different concentrations of fentanyl, tramadol, codeine, 6-MAM, and heroin, with corresponding concentrations and compound mass per spot presented. Proposed structures of uncommon deprotonated ions: B, [tramadol – H]⁺; C, [codeine – H]⁺; D, [6-MAM – H]⁺; E, [heroin – H]⁺.

The following analyzed compound was heroin, a semi-synthetic opioid. The $[\text{C}_{21}\text{H}_{23}\text{NO}_5 - \text{H}]^+$ ion was found in the five highest concentrations from 100 $\mu\text{g}/\text{mL}$ to 10 ng/mL . Limit of detection value for heroin was found to be 8.22 ng/mL (4.11 pg/spot). As seen in Figure 5G, the coefficient of determination R^2 was 0.86. In a study conducted in 2020 by Jovanov et al.,⁴⁶ which presented a rapid method for detecting heroin using HPLC–MS/MS, an LOD and LOQ were obtained from calibration curves of a 0.4 $\mu\text{g}/\text{mL}$ heroin standard solution.

The regression analysis of tramadol, a synthetic opioid produced as pain medication, was also based on its $[\text{M} - \text{H}]^+$ ion. Signals of significant intensity were found in the five highest concentrations, as presented in Figure 5H. LOD was calculated

and found to be 44.55 ng/mL (22.28 pg/spot), and the R^2 coefficient was determined to be 0.99. Abdelshakour et al.⁴⁷ conducted a study utilizing UPLC–MS/MS to quantify tramadol in methanol-diluted standard solutions. They achieved a limit of detection (LOD) of 0.015 $\mu\text{g}/\text{mL}$ and a limit of quantification (LOQ) of 0.05 $\mu\text{g}/\text{mL}$ for tramadol, with an R^2 value of 0.9999.

The last analyzed compound was methadone, also a synthetic opioid, often used for heroin addiction treatment. For this opioid, only the $[\text{C}_{21}\text{H}_{27}\text{NO} + \text{H}]^+$ ion has shown linear regression in terms of intensity and concentration relationship, as presented in Figure 4I. It was identified for the three highest concentrations, in the 100 $\mu\text{g}/\text{mL}$ to 1 $\mu\text{g}/\text{mL}$ range. The calculated LOD value was 386 ng/mL (193 pg/spot). The

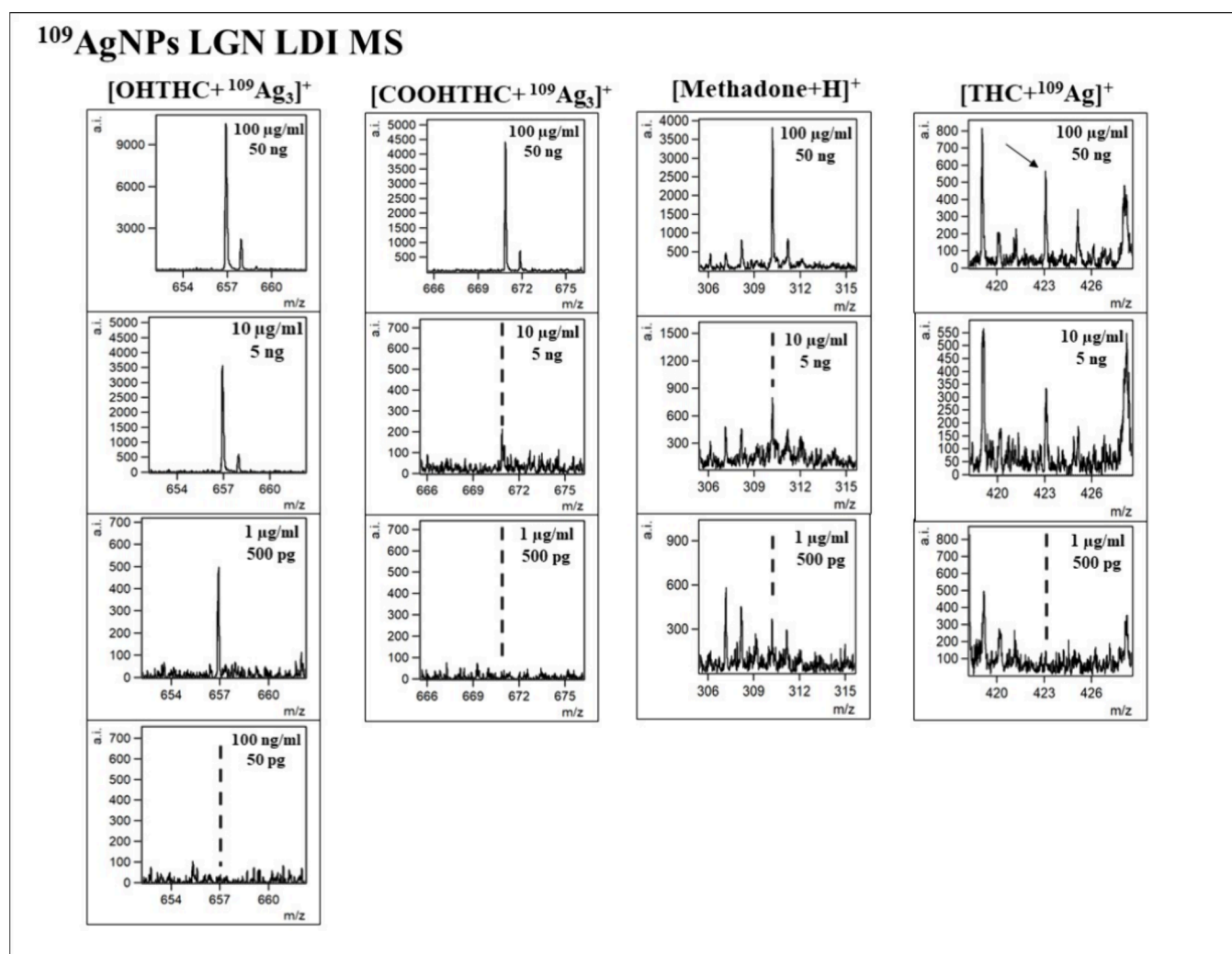


Figure 7. Spectra fragments for selected ions of interest presented for lowering concentrations for 11-OH-THC, 11-COOH-THC, methadone, and Δ^9 -THC with corresponding concentrations and compound weight per spot presented.

determination coefficient R^2 value was found to be 0.96. In research conducted by Whitehead et al.⁴⁸ in which the LC-MS/MS method was used to detect illicit drugs, the LOD and LOQ values determined for standard solutions were 3.8 pg/mL and 0.1 ng/mL, respectively.

3.2. Matrix Effect. Biological samples, such as tissues or body fluids, are considered to be a complex matrix containing, among others, proteins, peptides, lipids, and other endogenous compounds that may interfere with the detection of illicit drugs. This complexity often requires additional sample preparation steps, such as protein precipitation, solid-phase extraction, or liquid–liquid extraction, to isolate drugs from the biological matrix. Moreover, matrix effects in biological samples can affect the accuracy and sensitivity of detection methods. In contrast, our study, which uses standards diluted in methanol, avoids such matrix effects and can therefore demonstrate the capabilities of the analytical method in an idealized scenario. To validate the effectiveness of $^{109}\text{AgNPs}$ LGN LDI MS in the analysis of illicit drugs in complex mixtures such as biological samples, we conducted additional experiments on samples spiked with illicit drugs

The matrix effect was assessed by evaluating the ion intensity of fentanyl adducts. This involved comparing the intensity of ions from fentanyl in diluted urine and serum samples, which

had been spiked with standard compounds, against the ion intensity of corresponding adducts in pure standard solutions diluted in methanol (Figures S1 and S2, Supporting Information). The examination of signal intensities across the entire spectrum of tested fentanyl concentrations reveals that the adduct formed with silver-109 ions ($[\text{fentanyl} + ^{109}\text{Ag}]^+$) was the most prevalent ion species for this compound. This is evidenced by the significantly stronger signals for the silver adduct in comparison to those of the sodium ion adducts ($[\text{fentanyl} + \text{Na}]^+$) and the protonated fentanyl ions ($[\text{fentanyl} + \text{H}]^+$). The prominence of the silver adduct ion was consistent not only in the standard methanol solution but also in the diluted serum and urine samples. The LOD data indicate a high degree of method sensitivity for detecting fentanyl, both in the standard solution and in serum samples spiked with fentanyl, evidenced by LODs of 3.36 ± 0.68 pg/mL and 3.04 ± 0.81 pg/mL, respectively. For spiked urine, LOD was 4.05 ± 0.76 pg/mL. These surprisingly good results are probably results of 1000-times dilution of serum and urine, dilution that is needed in our method mainly due to the formation of thick films of material on the target plate. In this case it would be proper to recalculate LODs to include matrix dilution which gives 3.04 ± 0.81 and 4.05 ± 0.76 ng/mL for serum and urine, respectively. While biological matrix results are comparable to the ones from LCMS studies, still fentanyl LOD

for standard solution in methanol is among the lowest to date. Previously, Zhang et al. achieved one of the lowest reported LOD for fentanyl, reaching 2.5 ng/mL in diluted urine samples and 0.5 ng/mL in diluted blood samples, using a liquid chromatography–high resolution mass spectrometry.⁴⁹ Meanwhile, Busardo et al. recorded LOD values in the picogram per milliliter range for fentanyl, but with a lower resolution triple quadrupole mass spectrometer.⁵⁰ However, both studies involved complicated and time-consuming sample preparation processes, including protein precipitation, that were considerably more time-intensive compared to our rapid method.

3.3. Advantages and Disadvantages of ¹⁰⁹AgNPs LGN LDI MS. The laser desorption/ionization mass spectrometry method using silver-109 nanoparticles (¹⁰⁹AgNPs-LDI-MS) we've introduced offers considerable advantages over the commonly used atmospheric pressure ionization techniques in toxicological analyses and the detection of new psychoactive substances. A primary benefit of ¹⁰⁹AgNPs LGN LDI MS is its capacity for rapid analysis: up to 100 samples on a single 4.5 × 3.5 cm plate; the spectrum is ready typically within seconds per sample, with the potential for automation. This capability significantly enhances throughput. Unlike LC-MS methods, ¹⁰⁹AgNPs-LDI-MS is much less affected by matrix effects, reducing sample preparation time. For small molecular analyses in complex biological matrices such as blood or urine, a simple dilution suffices, eliminating the need for elaborate extraction and protein precipitation. While LC-MS often struggles with matrix effects leading to variable reproducibility, ¹⁰⁹AgNPs LGN LDI MS achieves superior sensitivity compared to other high-resolution methods under atmospheric pressure. On the other hand, high-performance liquid chromatography coupled with high-resolution mass spectrometry (UHPLC-HRMS) offers a robust advantage for the comprehensive and selective analysis of complex biological mixtures. By separating sample components on a chromatographic column before mass spectrometric analysis, UHPLC-HRMS is essential for the precise identification and quantification of chemical compounds within samples of complex composition. However, the LC-MS method is notably vulnerable to sample contamination; depending on the nature of the sample, contaminants could be introduced, potentially leading to the blockage of columns or tubing. Furthermore, the process of optimizing experimental conditions for LC-MS can be time-intensive, posing challenges when rapid analysis of numerous samples with minute analyte quantities is required. Additionally, sample availability often constrains LC-MS, particularly when the analyte of interest is unidentified and occurs in small amounts in the sample, making it challenging to ascertain the appropriateness of a specific dilution for detection.

4. CONCLUSION

LDI MS with the application of laser-generated silver-109-nanoparticles enabled the detection and quantification of illicit drugs in a broad range of concentrations, from 100 µg/mL to 100 pg/mL in the case of fentanyl. Analyzed standards produced typical adduct ions such as protonated, sodiated ions, and also ions specific to this method, adducts of ¹⁰⁹Ag⁺, and also less known [M + ¹⁰⁹Ag₃]⁺ and uncommon [M – H]⁺ ions. The chosen method turned out to be most suitable for rapid screening for fentanyl, resulting in a low limit of detection, giving exceptional results compared to other published reports. It is therefore a suitable analytical method for the detection and quantification of illicit drug occurrence and use.

■ ASSOCIATED CONTENT

Data Availability Statement

The data sets generated during and/or analyzed during the current study are available from the corresponding author upon request and in the RepOD open data repository (doi: 10.18150/EJLW9K).

Supporting Information

The Supporting Information is available free of charge at <https://pubs.acs.org/doi/10.1021/jasms.3c00454>.

Bar graphs showing the relationship between the log intensity of adduct ions and the log concentration of fentanyl in various samples: a methanol standard and diluted serum and urine. Spectra fragments displaying fentanyl ion signals in a standard solution and in fentanyl-spiked diluted serum and urine (PDF)

■ AUTHOR INFORMATION

Corresponding Author

Joanna Nizioł – Rzeszów University of Technology, Faculty of Chemistry, 35-959 Rzeszów, Poland; orcid.org/0000-0002-4783-8615; Phone: (+48 17) 865-1310; Email: jnizioł@prz.edu.pl

Author

Zuzanna Krupa – Doctoral School of Engineering and Technical Sciences at the Rzeszów University of Technology, 35-959 Rzeszów, Poland; Rzeszów University of Technology, Faculty of Chemistry, 35-959 Rzeszów, Poland

Complete contact information is available at: <https://pubs.acs.org/10.1021/jasms.3c00454>

Author Contributions

Conceptualization: J.N.; data curation: Z.K., J.N.; formal analysis: Z.K.; funding acquisition: J.N.; methodology: J.N., Z.K.; writing - original draft: Z.K.; writing - review and editing: J.N.. All authors read and agreed to the accepted version of the manuscript.

Notes

The authors declare no competing financial interest.

■ ACKNOWLEDGMENTS

The study was supported by National Science Centre (Poland) research project SONATA BIS number 2022/46/E/ST4/00016.

■ REFERENCES

- (1) United Nations Office on Drugs and Crime. *Prevalence of drug use. World Drug Report*. <https://dataunodc.un.org/dp-drug-use-prevalence> (accessed 2023-12-23).
- (2) Peacock, A.; Leung, J.; Larney, S.; Colledge, S.; Hickman, M.; Rehm, J.; Giovino, G. A.; West, R.; Hall, W.; Griffiths, P.; Ali, R.; Gowing, L.; Marsden, J.; Ferrari, A. J.; Grebely, J.; Farrell, M.; Degenhardt, L. Global Statistics on Alcohol, Tobacco and Illicit Drug Use: 2017 Status Report. *Addiction* **2018**, *113* (10), 1905–1926.
- (3) Duke-Novakowski, T. Opioids. *Pain Management in Veterinary Practice* **2013**, 39–67.
- (4) Volpe, D. A.; Tobin, G. A. M. M.; Mellon, R. D.; Katki, A. G.; Parker, R. J.; Colatsky, T.; Kropp, T. J.; Verbois, S. L. Uniform Assessment and Ranking of Opioid Mu Receptor Binding Constants for Selected Opioid Drugs. *Regul. Toxicol. Pharmacol.* **2011**, *59* (3), 385–390.

- (5) Hedegaard, H.; Miniño, A. M.; Warner, M. Key Findings Data from the National Vital Statistics System, Mortality. NCHS Data Brief No. 428, December 2021.
- (6) Spencer, M. R.; Miniño, A. M.; Warner, M. Drug Overdose Deaths in the United States, 2001–2021. Key Findings Data from the National Vital Statistics System. NCHS Data Brief No. 457, December 2022.
- (7) EMCDDA. New Psychoactive Substances - the Current Situation in Europe (European Drug Report 2023). https://www.emcdda.europa.eu/publications/european-drug-report/2023/new-psychoactive-substances_en#level-3-section1, 2023.
- (8) Grotenhermen, F.; Russo, E. *Cannabis and Cannabinoids: Pharmacology, Toxicology, and Therapeutic Potential*; Taylor & Francis, 2013; pp 1–439
- (9) Wall, M. E.; Perez-Reyes, M. The Metabolism of Δ^9 -Tetrahydrocannabinol and Related Cannabinoids in Man. *Journal of Clinical Pharmacology* **1981**, *21* (S1), 178S–189S.
- (10) Whitacre, D. M. *Reviews of Environmental Contamination and Toxicology*; Springer, 2011; Vol. 210. DOI: 10.1007/978-1-4419-7615-4.
- (11) Zuccato, E.; Castiglioni, S. Assessing Illicit Drug Consumption by Wastewater Analysis: History, Potential, and Limitation of a Novel Approach. *Illicit Drugs in the Environment: Occurrence, Analysis, and Fate Using Mass Spectrometry* **2011**, 291–304.
- (12) de Voogt, P.; Emke, E.; Helmus, R.; Panteliadis, P.; van Leerdam, J. A. Determination of Illicit Drugs in the Water Cycle by LC-Orbitrap MS. *Illicit Drugs in the Environment: Occurrence, Analysis, and Fate Using Mass Spectrometry* **2011**, 87–114.
- (13) Plouffe, B. D.; Murthy, S. K. Fluorescence-Based Lateral Flow Assays for Rapid Oral Fluid Roadside Detection of Cannabis Use. *Electrophoresis* **2017**, *38* (3–4), 501–506.
- (14) Parrilla, M.; Joosten, F.; De Wael, K. Enhanced Electrochemical Detection of Illicit Drugs in Oral Fluid by the Use of Surfactant-Mediated Solution. *Sens Actuators B Chem.* **2021**, *348*, 130659.
- (15) De Jong, M.; Slegers, N.; Kim, J.; Van Durme, F.; Samyn, N.; Wang, J.; De Wael, K. Electrochemical Fingerprint of Street Samples for Fast On-Site Screening of Cocaine in Seized Drug Powders. *Chem. Sci.* **2016**, *7* (3), 2364–2370.
- (16) Plaza, A.; Kołodziej, A.; Nizioł, J.; Ruman, T. Laser Ablation Synthesis in Solution and Nebulization of Silver-109 Nanoparticles for Mass Spectrometry and Mass Spectrometry Imaging. *ACS Measurement Science Au* **2022**, *2* (1), 14–22.
- (17) Arendowski, A.; Ruman, T. Lysine Detection and Quantification by Laser Desorption/Ionization Mass Spectrometry on Gold Nanoparticle-Enhanced Target. *Analytical Methods* **2018**, *10* (45), 5398–5405.
- (18) Arendowski, A.; Nizioł, J.; Ruman, T. Silver-109-Based Laser Desorption/Ionization Mass Spectrometry Method for Detection and Quantification of Amino Acids. *Journal of Mass Spectrometry* **2018**, *53* (4), 369–378.
- (19) Plaza-Altamer, A.; Kołodziej, A.; Nizioł, J.; Ruman, T. Infrared Pulsed Fiber Laser-Produced Silver-109-Nanoparticles for Laser Desorption/Ionization Mass Spectrometry of Amino Acids. *J. Mass Spectrom.* **2022**, *57* (3), No. 4815, DOI: 10.1002/jms.4815.
- (20) Kołodziej, A.; Plaza-Altamer, A.; Nizioł, J.; Ruman, T. Infrared Pulsed Fiber Laser-Produced Silver-109-Nanoparticles for Laser Desorption/Ionization Mass Spectrometry of Carboxylic Acids. *Int. J. Mass Spectrom.* **2022**, *474*, 116816.
- (21) Kołodziej, A.; Plaza-Altamer, A.; Nizioł, J.; Ruman, T. Infrared Pulsed Fiber Laser-Produced Silver-109 Nanoparticles for Laser Desorption/Ionization Mass Spectrometry of 3-Hydroxycarboxylic Acids. *Rapid Commun. Mass Spectrom.* **2022**, *36* (21), No. 9375, DOI: 10.1002/rcm.9375.
- (22) Kołodziej, A.; Ruman, T.; Nizioł, J. Gold and Silver Nanoparticles-Based Laser Desorption/Ionization Mass Spectrometry Method for Detection and Quantification of Carboxylic Acids. *Journal of Mass Spectrometry* **2020**, *55* (10), No. e4604.
- (23) Ciunik, Z.; Ruman, T.; Lukasiewicz, M.; Wolowiec, S. Complexes of Heteroscorpionate Trispyrazolylborate Ligands. Part XI. Weak CH/ π Interactions in Crystals of Hydrotris(3-Phenylpyrazolyl)-Boratothallium(I) and Hydrobis(5-Methyl-3-Phenylpyrazolyl)(3,5-Dimethylpyrazol-yl)Boratothallium(I) Studied by X-Ray Crystallography. *J. Mol. Struct.* **2004**, *690* (1–3), 175–180.
- (24) Nizioł, J.; Copié, V.; Tripet, B. P.; Nogueira, L. B.; Nogueira, K. O. P. C.; Ossoliński, K.; Arendowski, A.; Ruman, T. Metabolomic and Elemental Profiling of Human Tissue in Kidney Cancer. *Metabolomics* **2021**, *17* (3), 30.
- (25) Plaza-Altamer, A.; Kołodziej, A.; Krupa, Z.; Nizioł, J.; Ruman, T. Infrared Pulsed Fiber Laser-Produced Gold and Silver-109 Nanoparticles for Laser Desorption/Ionization Mass Spectrometry of Steroid Hormones. *Rapid Commun. Mass Spectrom.* **2023**, *37* (20), No. e9621.
- (26) Szulc, J.; Machnowski, W.; Kowalska, S.; Jachowicz, A.; Ruman, T.; Steglińska, A.; Gutarowska, B. Beeswax-Modified Textiles: Method of Preparation and Assessment of Antimicrobial Properties. *Polymers* **2020**, Vol. 12, Page 344 **2020**, *12* (2), 344.
- (27) Szulc, J.; Ruman, T.; Karbowska-Berent, J.; Koziellec, T.; Gutarowska, B. Analyses of Microorganisms and Metabolites Diversity on Historic Photographs Using Innovative Methods. *J. Cult Herit* **2020**, *45*, 101–113.
- (28) Szulc, J.; Kołodziej, A.; Ruman, T. Silver-109/Silver/Gold Nanoparticle-Enhanced Target Surface-Assisted Laser Desorption/Ionization Mass Spectrometry—The New Methods for an Assessment of Mycotoxin Concentration on Building Materials. *Toxins* **2021**, Vol. 13, Page 45 **2021**, *13* (1), 45.
- (29) Arendowski, A.; Szulc, J.; Nizioł, J.; Gutarowska, B.; Ruman, T. Metabolic Profiling of Moulds with Laser Desorption/Ionization Mass Spectrometry on Gold Nanoparticle Enhanced Target. *Anal. Biochem.* **2018**, *549*, 45.
- (30) Nizioł, J.; Ossoliński, K.; Tripet, B. P.; Copié, V.; Arendowski, A.; Ruman, T. Nuclear Magnetic Resonance and Surface-Assisted Laser Desorption/Ionization Mass Spectrometry-Based Serum Metabolomics of Kidney Cancer. *Anal Bioanal Chem.* **2020**, *412* (23), 5827.
- (31) Nizioł, J.; Ossoliński, K.; Tripet, B. P.; Copié, V.; Arendowski, A.; Ruman, T. Nuclear Magnetic Resonance and Surface-Assisted Laser Desorption/Ionization Mass Spectrometry-Based Metabolome Profiling of Urine Samples from Kidney Cancer Patients. *J. Pharm. Biomed Anal.* **2021**, *193*, 113752.
- (32) Misiorek, M.; Sekula, J.; Ruman, T. Mass Spectrometry Imaging of Low Molecular Weight Compounds in Garlic (*Allium Sativum* L.) with Gold Nanoparticle Enhanced Target. *Phytochemical Analysis* **2017**, *28* (6), 479–486.
- (33) Nizioł, J.; Sekula, J.; Ruman, T. Visualizing Spatial Distribution of Small Molecules in the Rhubarb Stalk (*Rheum Rhabarbarum*) by Surface-Transfer Mass Spectrometry Imaging. *Phytochemistry* **2017**, *139*, 72.
- (34) Nizioł, J.; Sunner, J.; Beech, I.; Ossoliński, K.; Ossolińska, A.; Ossoliński, T.; Plaza, A.; Ruman, T. Localization of Metabolites of Human Kidney Tissue with Infrared Laser-Based Selected Reaction Monitoring Mass Spectrometry Imaging and Silver-109 Nanoparticle-Based Surface Assisted Laser Desorption/Ionization Mass Spectrometry Imaging. *Anal. Chem.* **2020**, *92* (6), 4251–4258.
- (35) Ossoliński, K.; Ruman, T.; Ossoliński, T.; Ossolińska, A.; Arendowski, A.; Kołodziej, A.; Plaza-Altamer, A.; Nizioł, J. Monoisotopic Silver Nanoparticles-Based Mass Spectrometry Imaging of Human Bladder Cancer Tissue: Biomarker Discovery. *Adv. Med. Sci.* **2023**, *68* (1), 38–45.
- (36) Arendowski, A.; Nizioł, J.; Ossoliński, K.; Ossolińska, A.; Ossoliński, T.; Dobrowolski, Z.; Ruman, T. Laser Desorption/Ionization MS Imaging of Cancer Kidney Tissue on Silver Nanoparticle-Enhanced Target. *Bioanalysis* **2018**, *10* (2), 83–94.
- (37) Lou, X.; Spiering, A. J. H.; De Waal, B. F. M.; Van Dongen, J. L. J.; Vekemans, J. A. J. M.; Meijer, E. W. Dehydrogenation of Tertiary Amines in Matrix-Assisted Laser Desorption/Ionization Time-of-Flight Mass Spectrometry. *Journal of Mass Spectrometry* **2008**, *43* (8), 1110–1122.
- (38) Kang, C.; Zhou, Y.; Du, Z.; Bian, Z.; Wang, J.; Qiu, X.; Gao, L.; Sun, Y. Dehydrogenation and Dehalogenation of Amines in MALDI-TOF MS Investigated by Isotopic Labeling. *Journal of Mass Spectrometry* **2013**, *48* (12), 1318–1324.

(39) Prysiashnyi, V.; Dycka, F.; Kratochvil, J.; Stranak, V. Gas Aggregated Ag NPs as a Matrix for Small Molecules: A Study on Natural Amino Acids. *J. Nanopart. Res.* **2020**, *22* (11), 1–13.

(40) Kéki, S.; Nagy, L.; Deák, G.; Zsuga, M.; Somogyi, L.; Lévai, A. Cationization of Simple Organic Molecules by Singly-Charged Ag₃⁺ Cluster Ions in Matrix-Assisted Laser Desorption/Ionization Mass Spectrometry: Metal Cluster-Molecule Interactions. *J. Am. Soc. Mass Spectrom.* **2004**, *15* (6), 879–883.

(41) Nizioł, J.; Rode, W.; Laskowska, B.; Ruman, T. Novel Monoisotopic ¹⁰⁹AgNPET for Laser Desorption/Ionization Mass Spectrometry. *Anal. Chem.* **2013**, *85* (3), 1926–1931.

(42) Angi, C.; Lurie, I. S.; Marginean, I. Analysis of Fentanyl Derivatives by Ultra High Performance Liquid Chromatography with Diode Array Ultraviolet and Single Quadrupole Mass Spectrometric Detection. *J. Sep. Sci.* **2019**, *42* (9), 1686–1694.

(43) Heo, S.; Yoo, G. J.; Choi, J. Y.; Park, H. J.; Do, J. A.; Cho, S.; Baek, S. Y.; Park, S. K. Simultaneous Analysis of Cannabinoid and Synthetic Cannabinoids in Dietary Supplements Using UPLC with UV and UPLC-MS-MS. *J. Anal. Toxicol.* **2016**, *40* (5), 350–359.

(44) Simões, S. S.; Ajenjo, A. C.; Dias, M. J. Qualitative and Quantitative Analysis of THC, 11-Hydroxy-THC and 11-nor-9-Carboxy-THC in Whole Blood by Ultra-Performance Liquid Chromatography/Tandem Mass Spectrometry. *Rapid Commun. Mass Spectrom.* **2011**, *25* (18), 2603–2610.

(45) Gul, W.; Stamper, B.; Godfrey, M.; Gul, S. W.; Elsohly, M. A. LC-MS-MS Method for Analysis of Opiates in Wastewater During Football Games II. *J. Anal. Toxicol.* **2016**, *40* (5), 330–337.

(46) Jovanov, P.; Petrin-Miličević, M.; Radosavljević-Stevanović, N.; Vraneš, M.; Belić, S.; Sakač, M.; Nikolov, J.; Gađžurić, S. Rapid Determination of the Primary Alkaloids in Illicit Heroin by High-Performance Liquid Chromatography with Tandem Mass Spectrometry (HPLC-MS/MS). *Anal. Lett.* **2021**, *54* (7), 1224–1232.

(47) Abdelshakour, M. A.; Hadad, G. M.; Abdel Salam, R. A.; Abo-ElMatty, D. M.; Abdel Hameed, E. A. HPLC and UPLC-MS/MS Methods for Analyzing TRAMADOL in 70 Medicinal Illegal Products: Application to Counterfeit Study. *Microchemical Journal* **2021**, *161*, 105823.

(48) Whitehead, H. D.; Hayes, K. L.; Swartz, J. A.; Prete, E.; Robison-Taylor, L.; Ellen Mackesy-Amiti, M.; Jimenez, A. D.; Lieberman, M. Validated Method for the Analysis of 22 Illicit Drugs and Their Metabolites via Liquid Chromatography Tandem Mass Spectrometry (LC-MS/MS) in Illicit Drug Samples Collected in Chicago, IL. *Forensic Chemistry* **2023**, *33*, 100475.

(49) Zhang, Y.; Halifax, J. C.; Tangsombatvisit, C.; Yun, C.; Pang, S.; Hooshfar, S.; Wu, A. H. B.; Lynch, K. L. Development and Application of a High-Resolution Mass Spectrometry Method for the Detection of Fentanyl Analogs in Urine and Serum. *Journal of Mass Spectrometry and Advances in the Clinical Lab* **2022**, *26*, 1–6.

(50) Busardò, F. P.; Carlier, J.; Giorgetti, R.; Tagliabracci, A.; Pacifici, R.; Gottardi, M.; Pichini, S. Ultra-High-Performance Liquid Chromatography-Tandem Mass Spectrometry Assay for Quantifying Fentanyl and 22 Analogs and Metabolites in Whole Blood, Urine, and Hair. *Front. Chem.* **2019**, *7* (APR), 447886.